Published in final edited form as:
J Neural Transm. 2008 December ; 115(12): 1661–1671. doi:10.1007/s00702-008-0137-1.

Fine structural analysis of the neuronal inclusions of frontotemporal lobar degeneration with TDP-43 proteinopathy

Julian R. Thorpe,
Electron Microscope Division, The Sussex Centre for Advanced Microscopy, John Maynard-Smith Building, School of Life Sciences, University of Sussex, Falmer, Brighton, East Sussex BN1 9QG, UK

Helen Tang,
Electron Microscope Division, The Sussex Centre for Advanced Microscopy, John Maynard-Smith Building, School of Life Sciences, University of Sussex, Falmer, Brighton, East Sussex BN1 9QG, UK

Joe Atherton, and
Electron Microscope Division, The Sussex Centre for Advanced Microscopy, John Maynard-Smith Building, School of Life Sciences, University of Sussex, Falmer, Brighton, East Sussex BN1 9QG, UK

Nigel J. Cairns
Alzheimer's Disease Research Center, Departments of Neurology and Pathology and Immunology, Washington University School of Medicine, St Louis, MI 63110, USA

Julian R. Thorpe: j.r.thorpe@sussex.ac.uk; Helen Tang: ; Joe Atherton: ; Nigel J. Cairns:

Abstract

TAR DNA-binding protein of 43 kDa (TDP-43) is a major component of the pathological inclusions of frontotemporal lobar degeneration with TDP-43 proteinopathy, also called FTLD with ubiquitin-positive, tau-negative inclusions (FTLD-U), and motor neuron disease (MND). TDP-43 is predominantly expressed in the nucleus and regulates gene expression and splicing. In FTLD with TDP-43 proteinopathy, neuronal inclusions present variably as cytoplasmic inclusions (NCIs), dystrophic neurites (DNs), and intranuclear inclusions (NIIs), leading to a fourfold neuropathological classification correlating with genotype. There have been few fine structural studies of these inclusions. Thus, we undertook an immunoelectron microscopic study of FTLD with TDP-43 proteinopathy, including sporadic and familial cases with *progranulin* (*GRN*) mutation. TDP-43-immunoreactive inclusions comprised two components: granular and filamentous. Filament widths, expressed as mean (range) were: NCI, 9 nm (4–16 nm); DN, 10 nm (5–16 nm); NII, 18 nm (9–50 nm). Morphologically distinct inclusion components may reflect the process of TDP-43 aggregation and interaction with other proteins: determining these latter may contribute towards understanding the heterogeneous pathogenesis of FTLD with TDP-43 proteinopathy.

Keywords

Frontotemporal lobar degeneration; Ubiquitin; TDP-43; TARDBP; Progranulin; Immunoelectron microscopy

Correspondence to: Julian R. Thorpe, j.r.thorpe@sussex.ac.uk.

Introduction

TAR DNA-binding protein of 43 kDa (TDP-43) is a major component of the inclusions of frontotemporal lobar degeneration with TDP-43 proteinopathy, also called FTLD with ubiquitin-immunoreactive, tau-negative inclusions (FTLD-U), FTLD-U with motor neuron disease (FTLD-MND), and MND (Cairns et al. 2007a; Neumann et al. 2006). TDP-43 is also being recognised increasingly as a variable component of inclusions of other neurodegenerative diseases including Alzheimer's disease (AD) (Amador-Ortiz et al. 2007), corticobasal degeneration (Uryu et al. 2008), dementia with Lewy bodies (Higashi et al. 2007; Nakashima-Yasuda et al. 2007), ALS/dementia-parkinsonism of Guam (Geser et al. 2008), and hippocampal sclerosis (Amador-Ortiz et al. 2007). In FTLD with TDP-43 proteinopathy, three types of neuronal TDP-43-immunoreactive inclusions have been described: neuronal cytoplasmic inclusions (NCIs), dystrophic neurites (DNs) and neuronal intranuclear inclusions (NIIs). In FTLD-MND, TDP-43 aggregates may be present, additionally, in glial cells (Brandmeir et al. 2008; Seelaar et al. 2007), most commonly in oligodendrocytes, but the inclusions in FTLD-MND are distinct from the Papp-Lantos bodies of multiple system atrophy where the major pathological protein is α-synuclein (Jellinger 2003); in contrast, the glial cytoplasmic inclusions (GCIs) of FTLD-MND are TDP-43-immunoreactive and α-synuclein-negative. In addition to the distinct immunohistochemical profile of the inclusions of FTLD and MND with TDP-43 proteinopathy, this group of diseases is characterised by a unique biochemical signature: TDP-43 forms relatively insoluble aggregates that are ubiquitinated and hyperphosphorylated and cleaved to generate abnormal C-terminal fragments which may be visualised by immunoblotting (Neumann et al. 2006).

TDP-43 was initially cloned and characterised as a protein that binds to human immunodeficiency virus type-1 (HIV1) TAR DNA-sequence motifs (Ignatius et al. 1995). It is predominantly expressed within the nucleus and is encoded by the *TAR DNA-binding protein* (*TARDBP*) gene on chromosome 1. The functional repertoire of TDP-43 is incompletely known but includes regulation of gene expression and mRNA splicing (Ayala et al. 2005; Buratti and Baralle 2001). TDP-43 has two mRNA-binding domains, a heterogeneous ribonucleoprotein (hnRNP) binding site, and nuclear localisation and export motifs. TDP-43 has been implicated in the pathogenesis of cystic fibrosis via transcriptional repression and exon skipping (Buratti et al. 2001, 2004, 2005; Zuccato et al. 2004).

TDP-43 proteinopathy is clinically heterogeneous and includes the spectrum of phenotypes encompassed by FTLD, FTLD-MND and MND; additionally, the memory deficits more commonly seen in dementia of the Alzheimer's type, parkinsonism, and corticobasal syndrome may be present. In addition to sporadic cases, there is also molecular genetic heterogeneity. FTLD with TDP-43 proteinopathy may be caused by mutations in several genes: FTLD with *progranulin* (*GRN*) mutation, FTLD with *valosin-containing protein* (*VCP*) mutation, and FTLD-linked chromosome 9 (Cairns et al. 2007a). Recently, mutations were reported in the *TARDBP* gene in autosomal dominantly inherited MND (Gitcho et al. 2008; Kabashi et al. 2008; Sreedharan et al. 2008). These observations indicate that abnormal TDP-43 alone is sufficient to cause neuro-degeneration.

Although there have been several studies describing the morphology and immunoreactive profile of inclusions in FTLD with TDP-43 proteinopathy at the light microscope level (Arai et al. 2006; Cairns et al. 2007b; Davidson et al. 2007; Neumann et al. 2006), there have been only isolated and limited reports of the fine structure of the inclusions in the TDP-43 proteinopathies (Amador-Ortiz et al. 2007; Cairns et al. 2007b; Hasegawa et al. 2008). Therefore, to further characterise the inclusions of FTLD with TDP-43 proteinopathy, we have undertaken an immunoelectron microscopic study and show that there are, variably, two components to the inclusions: granular material and filamentous or fibrillary material. The

presence of these different components probably reflects the process of TDP-43 aggregation and the presence of partner proteins within the granular regions of inclusions in FTLD with TDP-43 proteinopathy.

Materials and methods

Brain tissue collection, processing, and neuropathological assessment

Frozen and formalin-fixed, paraffin wax-embedded brain tissues from clinically and neuropathologically well-characterised cases of FTLD with TDP-43 proteinopathy (Table 1) were obtained from the Alzheimer's Disease Research Center, Washington University School of Medicine, St. Louis, MI, USA. Tissues from the middle frontal gyrus of six cases were used for this study, including two cases of FTLD with *GRN* mutation which we reported previously (Mukherjee et al. 2006,2008). The pattern and distribution of inclusions in these cases was previously assessed using the Consensus Criteria for Frontotemporal Lobar Degeneration: three cases were FTLD-U type 2 and three cases were FTLD-U type 3 (Cairns et al. 2007a). Tissue was removed according to Washington University Local Ethics Committee guide-lines and informed consent for brain donation was obtained from the next-of-kin.

Histology and immunohistochemistry

Tissue blocks were taken from the middle frontal gyrus. Antigen retrieval was performed by heating sections in a solution of 0.5% ethylenediaminetetraacetic acid (EDTA) in 100 mmol/L Tris, pH 7.6 at 100°C for 10 min. Immunohistochemistry (IHC) was undertaken on 6–10 μm-thick sections prepared from formalin-fixed, paraffin wax-embedded tissue blocks using the avidin–biotin complex detection system (Vector Laboratories, Burlingame, CA, USA) and the chromagen 3,3′-diaminobenzidine (DAB) and sections were counterstained with haematoxylin. Antibodies used included those that recognise ubiquitin (1:2,000; Dako UK Ltd., Ely, UK) and TDP-43 (1:2,000, Proteintech Inc., Chicago, IL, USA). The antibodies used in this study are well-characterised and have been used previously to demonstrate epitopes of ubiquitin and TDP-43 in sporadic and familial cases of FTLD with TDP-43 proteinopathy (Cairns et al. 2007b). After the completion of this study, a disease-specific phosphorylation-dependent anti-TDP-43 antibody was reported (Hasegawa et al. 2008), but this was not available for the use in the experiments described here.

Tissue preparation for transmission electron microscopy

Frozen brain tissue stored at −70°C was brought to −20°C. The grey matter was identified, dissected, and samples placed directly into a cold (4°C) solution of 4% (w/v) formaldehyde and 0.1% (v/v) glutaraldehyde (vacuum-distilled) in phosphate-buffered saline (PBS). The following procedures were carried out at 4°C. After 18 h of fixation, the samples were rinsed thoroughly in PBS then dehydrated in an ethanol series and embedded in Unicryl resin (British BioCell International, Cardiff, UK) as previously described (Thorpe et al. 2001).

Primary antibodies and secondary probes

Affinity-purified polyclonal rabbit IgGs, raised against human recombinant TDP-43 protein and ubiquitin, were obtained from Proteintech Group, Inc. (Chicago, IL, USA) and Dako UK Ltd. (Ely, UK), respectively. A 10 nm gold particle-conjugated goat anti-rabbit IgG secondary probe (GaR10) was obtained from British BioCell International (Cardiff, UK).

Immunogold labelling transmission electron microscopy

We used established methods to perform immunogold transmission electron microscopy (TEM) (Thorpe 1999). A modified PBS, pH 8.2 containing 1% BSA, 500 μl/L Tween-20, 10 mM NaEDTA and 0.2 g/L NaN_3 (hence-forward termed PBS+) was used throughout all the

following procedures for all dilutions of antibodies and gold probes. For each of the six cases, three separate blocks of tissue were sectioned for immunogold labelling. Multiple serial sections were cut and collected on TEM support grids for immunolabelling. Serial sections were initially blocked in normal goat serum (1:10 in PBS+) for 30 min ambient. To investigate the fine structure of the inclusions, sections were single-labelled with anti-TDP-43 (2 μg/ml IgG final concentration) and anti-ubiquitin (25 μg/ml IgG final concentration). To determine the specificity of the anti-TDP-43 and anti-ubiquitin antibodies, control incubations were run using non-immune rabbit serum at IgG concentrations matching the concentrations of the primary antibodies.

After 3 × 2 min PBS+ rinses, the sections were immunolabelled in GaR10 (1:10) for 1 h ambient. Sections were subsequently rinsed in PBS+ (3 × 10 min) and distilled water (4 × 5 min). All immunogold labelled thin sections were post-stained in 0.5% (w/v) aqueous uranyl acetate for 1 h and examined in a Hitachi-7100 TEM at 100 kV. The sections were systematically thoroughly scanned for pathology and images acquired digitally with an axially mounted (2 × 2 K pixel) Gatan Ultrascan 1000 CCD camera (Gatan UK, Oxford, UK).

Results

Immunohistochemistry

At the light microscope level, TDP-43-immunoreactive inclusions were detected at three sites: NCIs, DNs, and rare NIIs (Fig. 1a, b, c); no glial inclusions were seen. In the six cases examined, NCIs and DNs were the most frequent morphological type; NIIs were rare in the familial cases of FTLD with *GRN* mutation and not seen in any of the sporadic cases. As previously reported, NCIs were present in neurons that lacked nuclear TDP-43-immunoreactivity, indicating a redistribution of the normally predominantly nuclear protein to abnormal cytoplasmic aggregates (Fig. 1c).

Neuronal nuclear localisation of TDP-43

Immunoelectron TEM of normal brain neurons revealed a predominantly nuclear localisation of TDP-43 consistent with that seen by IHC with the light microscope. TDP-43 labelling was preferentially associated with euchromatin regions within the nucleus (Fig. 2a, b).

Neuronal cytoplasmic inclusions

By TEM, TDP-43-labelled NCIs appeared typically oval or round and lacked a limiting membrane (Fig. 3a, d, respectively). The inclusions generally contained admixed granular and filamentous components (Fig. 3b, c). Some inclusions of a very granular appearance were more heavily immunolabelled with anti-TDP-43 antibodies (Fig. 3d). More rarely, the filamentous component predominated, although TDP-43 labelling was generally heavier over the more densely stained, granular regions of the inclusion (Fig. 3e, f; Table 3). Dispersed filaments within the NCIs had a mean diameter of 9 nm (range 4–16 nm; Table 2). Serial sections labelled with anti-ubiquitin and anti-TDP-43 antibodies revealed that the NCIs contained both ubiquitin (data not shown) and TDP-43 epitopes.

The TDP-43-positive inclusion-bearing neurons had very low levels of TDP-43 labelling within their nuclei, consistent with that observed with the light microscope (Fig. 1c). This loss of nuclear labelling was also observed in neurons with no apparent inclusion, most likely explained by only partial inclusion of the neuron in the plane of section. There was also labelling of loosely defined aggregates with anti-TDP-43 antibodies in perikaryal regions, a phenomenon which may be an early stage in the evolution of TDP-43-immunoreactive inclusions. This redirection of TDP-43 to the cytoplasm may be the harbinger of ubiquitination, proteolytic cleavage, and eventual aggregation to form a relatively insoluble protein aggregate.

For example, Fig. 4a and b show two neurons of similar appearance, with lipofuscin accumulations, and cytoplasm of a normal appearance; however, there were high levels of TDP-43 labelling in the nucleus and low levels in the cytoplasm of the neuron in Fig. 4a, whereas, the neuron in Fig. 4b, showed cytoplasmic relocation of TDP-43 protein (Fig. 4b), with concurrent low levels within the nucleus. Figure 4d shows another example of a neuron showing a perikaryal accumulation of TDP-43 within cytoplasm of a normal appearance, whilst the nucleus exhibits virtually no TDP-43 positivity. Also compare these levels of labelling with those of the normal brain neuronal nuclei in Fig. 2.

Dystrophic neurites

TDP-43-positive neuritic processes were observed in sections in four of the six cases examined. These varied greatly in morphology. Frequently, DNs appeared as narrow (200–300 nm wide) processes with a very ordered filamentous structure (Fig. 5); these filaments ranged in width from 5 to 16 nm, with a mean of 10 nm (Table 2). These latter DNs often appeared as very short processes, presumably reflecting their partial appearance in the plane of section.

Less frequently, TDP-43-positive processes were more swollen and dystrophic (~1–5 μm wide; Fig. 6). These DNs were characterised by either a dense, amorphous, granular content (Fig. 6a, b) or, more rarely, a filamentous component intermingled with the granular component (Fig. 6c, d; Table 3). In these mixed structures, more intense TDP-43 labelling was associated with the granular component (Fig. 6d). These swollen, TDP-43-positive DNs were also heavily ubiquitinated as demonstrated by labelling of serial sections labelled with anti-ubiquitin antibodies (Fig. 6e).

Neuronal intranuclear inclusion

NIIs are typically absent in FTLD with TDP-43 proteinopathy type 2, and are typically sparsely observed by light microscopy in type 3 cases (Cairns et al. 2007a). They are most frequently seen in cases of FTLD with *valosin-containing protein* (*VCP*) gene mutations (Cairns et al. 2007a), but none of these cases was available for immunogold TEM. Many grids were examined before we observed one well-defined NII by TEM (Fig. 7). The NII was initially identified by the presence of abnormal fibrils within the nucleus. Interestingly, this type of NII may not be immediately recognisable as an NII with the light microscope because the overall intensity of TDP-43 labelling was similar to that of normal brain nuclei. The recently described phosphorylation-dependent anti-TDP-43 antibody (Hasegawa et al. 2008) should greatly facilitate the identification of nuclear inclusions. The mean fibril diameter was 18 nm (range 9–50 nm). The broadest filaments were present in bundles, which were aligned with the nuclear envelope (Fig. 7a), and were relatively intensely labelled with anti-TDP-43 antibodies (Fig. 7b, d). These latter were at the periphery of the inclusion and encircled a region of medium- and fine-diameter fibrils that were associated with fine granular material. This granular material and the finer filaments were relatively lightly labelled (Fig. 7c; Table 2, Table 3).

Discussion

TDP-43 has recently been added to the list of proteins that are misfolded and progressively aggregate to form the hall-mark pathological inclusions of several neurodegenerative diseases (Armstrong et al. 2008). TDP-43 proteinopathy is the most recent molecular pathology to be added to this list. TDP-43 is the major pathological protein of the ubiquitin-positive, tau- and α-synuclein-negative inclusions of FTLD-U, FTLD-MND and MND (Neumann et al. 2006), and a variable component of the inclusions of an increasing number of other diseases, including AD (Amador-Ortiz et al. 2007), corticobasal degeneration (Uryu et al. 2008), dementia with Lewy bodies (Higashi et al. 2007; Nakashima-Yasuda et al. 2007) ALS/dementia-

parkinsonism of Guam (Geser et al. 2008), and hippocampal sclerosis (Amador-Ortiz et al. 2007).

The importance of TDP-43 was recently underscored by the discovery of missense mutations in the *TARDBP* gene (Gitcho et al. 2008; Kabashi et al. 2008; Sreedharan et al. 2008). These molecular genetic defects in affected individuals with autosomal dominantly inherited disease confirm that abnormal TDP-43 is sufficient to cause TDP-43 proteinopathy, neurodegeneration, and clinical symptoms. The biochemical signature of this group of diseases, called TDP-43 proteinopathies, is sarkosylinsoluble, urea-soluble TDP-43 which is ubiquitinated and forms abnormal C-terminal cleavage products which are also hyperphosphorylated (Arai et al. 2006; Hasegawa et al. 2008; Neumann et al. 2006). Theses biochemical changes correlate with the brain areas with TDP-43-immunoreactive aggregates. Insights into the in vivo aggregation and toxicity of TDP-43 have recently been acquired from a yeast model of TDP-43 proteinopathy (Johnson et al. 2008). Increased (full-length) TDP-43 expression resulted in cytoplasmic aggregation of the protein in the form of inclusions and their data established that TDP-43 had a cytotoxic effect in vitro. Expression of a range of DNA constructs also showed that the C-terminal region and one of the two RNA-recognition motifs (RRM2) were required to produce both cytoplasmic aggregation and a cytotoxic effect of TDP-43; these data, together with the causative mutations in TARDBP, implicate TDP-43 directly in the pathogenesis of TDP-43 proteinopathy.

In this study, we investigated the fine structure of three types of neuronal inclusions of sporadic and familial FTLD with TDP-43 proteinopathy using immunogold TEM. The NCIs and DNs of sporadic FTLD with TDP-43 proteinopathy were similar to those seen in familial FTLD with *GRN* mutation. Despite extensive searching of multiple grids, too few NIIs were identified to make a comparison between these two groups. To date, there have been very few ultrastructural studies of the inclusions of FTLD with TDP-43 proteinopathy. Amador-Ortiz et al. 2007 investigated TDP-43 in FTLD with TDP-43 proteinopathy within the setting of hippocampal sclerosis and AD. They reported, but showed no data of, TDP-43 epitopes within granular and filamentous NCIs and DNs of FTLD with TDP-43 proteinopathy cases; the filaments were straight and 15–20 nm in width. Interestingly, the diameter of fibrils made from recombinant TDP-43 was reported as 15 nm (Hasegawa et al. 2008), comparable to the filament width reported in this study.

In a large immunohistochemical investigation of TDP-43 in sporadic and familial cases of FTLD with ubiquitin-imunoreactive, tau-negative inclusions, TEM images revealed TDP-43 epitopes in a hippocampal NCI and a DN from the temporal lobe: the NCIs were predominantly granular with a minor filamentous component; in contrast, DNs were more filamentous in appearance (Cairns et al. 2007b).

In this report, we have extended our earlier studies (Cairns et al. 2007b) to include a detailed investigation of the fine structure of the neuronal inclusions of FTLD with TDP-43 proteinopathy. Initial observations of normal age-matched control cases showed the expected predominantly nuclear localisation of TDP-43; there was a similar TDP-43 distribution in unaffected neurons within the FTLD with TDP-43 proteinopathy cases. Nuclear TDP-43 immunolabelling was preferentially associated with regions of euchromatin, which is consistent with its known role in transcriptional regulation (Ayala et al. 2005; Buratti and Baralle 2001).

At the ultrastructural level, the inclusions within neuronal cytoplasmic (NCIs), neuritic (DNs) and nuclear compartments (NII) comprised both granular and fibrillar components. Within NCIs these granular and filamentous components were admixed, with the former being more heavily TDP-43-immunoreactive. Conversely, in the finer TDP-43-immunoreactive neurites

and in the NII frequent TDP-43 epitopes were identified with fibrils. Some of these filaments were broader in the nuclear compartment than any TDP-43-positive filaments observed in the NCIs or DNs. Interestingly, we showed previously that the filaments of NIIs of neuronal intermediate filament inclusion disease (NIFID) were broader than those of the NCIs (20 nm compared with 10 nm; Mosaheb et al. 2005). Whilst the granular component of the NII of FTLD with TDP-43 proteinopathy was relatively minor, this granular component predominated within most of the mature, swollen DNs and contained frequent TDP-43 epitopes.

The TEM ultrastructural method used in this study has not only elucidated the fine structure of the neuronal inclusions, but has also provided an insight into the process of TDP-43 aggregation which is not discernible with the light microscope. For example, we observed neurons with low levels of nuclear TDP-43 and significant perikaryal TDP-43 positivity over areas of cytoplasm of a normal appearance indicating that the redistribution of TDP-43 takes place at an early stage in the disease process, rather than being secondary to accumulation with other interacting proteins within the cytoplasm. This redistribution of TDP-43 is reminiscent of that of another nuclear protein, Pin1, which has multiple cellular roles, including transcriptional regulation, which we have previously shown to be redistributed to the cytoplasm of neurons in several FTLD entities (Thorpe et al. 2004). The loss of nuclear function of TDP-43 might be the stimulus for activation of an apoptotic cascade as has been suggested for Pin1 nuclear depletion. Further studies are required to elucidate the significance of translocation of TDP-43 between the nucleus and cytoplasm.

In addition, we have identified a predominantly filamentous NII. Importantly, this inclusion is unlikely to have been apparent by light microscopy as the overall level of nuclear TDP-43 was not significantly higher than of normal neuronal nuclei. TDP-43 immunolabelling specifically aligned along the broadest fibrils of the NII, but only at intermittent points. As the finer filaments were weakly TDP-43-immunoreactive, this suggests that TDP-43 may be recruited following a prior aggregation step, or TDP-43 is post-translationally modified differently in the nucleus compared to the cytoplasm, resulting in an altered immunoreactive profile.

Overall, this work contributes to our understanding of the ultrastructural morphology of TDP-43 inclusions, and complements and extends upon other such data published whilst this manuscript was under review (Lin and Dickson 2008). The full functional repertoire of TDP-43 and the identities of its interacting proteins are incompletely understood. The elucidation of the normal physiological role of TDP-43 is likely to illuminate possible mechanisms of pathogenesis. Also, the future use of disease-specific anti- TDP-43 antibodies and those of its partner proteins or nucleic acids should provide insights into the abnormal accumulation of TDP-43 in the nucleus, cytoplasm and neurite of the degenerating neuron of FTLD with TDP-43 proteinopathy.

Acknowledgments

We thank the families of patients whose generosity made this research possible. We acknowledge the staff of the Alzheimer's Disease Research Center Neuropathology Laboratory, Department of Pathology & Immunology, Washington University School of Medicine, St. Louis, USA and Max Allin, University of Sussex, for technical assistance. Support for this work was provided by grants from the Wellcome Trust, UK, (GR066166AIA) to JRT and NJC, and the National Institute on Aging of the National Institutes of Health (P50 AG05681 and P01 AG03991) to NJC.

References

Amador-Ortiz CLW, Ahmed Z, Personett D, et al. TDP-43 immunoreactivity in hippocampal sclerosis and Alzheimer's disease. Ann Neurol 2007;61:435–445. [PubMed: 17469117]

Arai T, Hasegawa M, Akiyama H, et al. TDP-43 is a component of ubiquitin-positive tau-negative inclusions in frontotemporal lobar degeneration and amyotrophic lateral sclerosis. Biochem Biophys Res Commun 2006;351:602–611. [PubMed: 17084815]

Armstrong RAL, Lantos PL, Cairns NJ. What determines the molecular composition of abnormal protein aggregates in neurodegenerative disease? Neuropathology. 2008PM:18433435

Ayala YM, Pantano S, D'Ambrogio A, et al. Human, Drosophila, and *C elegans* TDP 43: nucleic acid binding properties and splicing regulatory function. J Mol Biol 2005;348:575–588. [PubMed: 15826655]

Brandmeir NJ, Geser F, Kwong LK, et al. Severe subcortical TDP-43 pathology in sporadic frontotemporal lobar degeneration with motor neuron disease. Acta Neuropathol 2008;115:123–131. [PubMed: 18004574]

Buratti E, Baralle FE. Characterization and functional implications of the RNA binding properties of nuclear factor TDP-43, a novel splicing regulator of CFTR exon 9. J Biol Chem 2001;276:36337–36343. [PubMed: 11470789]

Buratti E, Dork T, Zuccato E, Pagani F, Romano M, Baralle FE. Nuclear factor TDP-43 and SR proteins promote in vitro and in vivo CFTR exon 9 skipping. EMBO J 2001;20:1774–1784. [PubMed: 11285240]

Buratti E, Brindisi A, Pagani F, Baralle FE. Nuclear factor TDP-43 binds to the polymorphic TG repeats in CFTR intron 8 and causes skipping of Exon 9: a functional link with disease penetrance. Am J Hum Genet 2004;74:1322–1325. [PubMed: 15195661]

Buratti E, Brindisi A, Giombi M, Tisminetzky S, Ayala YM, Baralle FE. TDP-43 binds heterogeneous nuclear ribonucleoprotein A/B through its C-terminal tail—An important region for the inhibition of cystic fibrosis transmembrane conductance regulator exon 9 splicing. J Biol Chem 2005;280:37572–37584. [PubMed: 16157593]

Cairns NJ, Bigio EH, Mackenzie IRA, et al. Neuropathologic diagnostic and nosologic criteria for frontotemporal lobar degeneration: consensus of the Consortium for Frontotemporal Lobar Degeneration. Acta Neuropathol 2007a;114:5–22. [PubMed: 17579875]

Cairns NJ, Neumann M, Bigio EH, et al. TDP-43 in familial and sporadic frontotemporal lobar degeneration with ubiquitin inclusions. Am J Pathol 2007b;171:227–240. [PubMed: 17591968]

Davidson Y, Kelley T, Mackenzie IRA, et al. Ubiquitinated pathological lesions in frontotemporal lobar degeneration contain the TAR DNA-binding protein, TDP-43. Acta Neuropathol 2007;113:521–533. [PubMed: 17219193]

Geser F, Winton MJ, Kwong LK, et al. Pathological TDP-43 in parkinsonism-dementia complex and amyotrophic lateral sclerosis of Guam. Acta Neuropathol 2008;115:133–145. [PubMed: 17713769]

Gitcho MA, Baloh RH, Chakraverty S, et al. TDP-43 A315T mutation in familial motor neuron disease. Ann Neurol 2008;63:535–538. [PubMed: 18288693]

Hasegawa MAT, Nonaka T, Kametani F, et al. Phosphorylated TDP-43 in frontotemporal lobar degeneration and amyotrophic lateral sclerosis. Ann Neurol 2008;64:60–70. [PubMed: 18546284]

Higashi S, Iseki E, Yamamoto R, et al. Concurrence of TDP-43, tau and alpha-synuclein pathology in brains of Alzheimer's disease and dementia with Lewy bodies. Brain Res 2007;1184:284–294. [PubMed: 17963732]

Ignatius SH, Wu F, Harrich D, Garciamartinez LF, Gaynor RB. Cloning and characterization of a novel cellular protein, TDP-43, that binds to human-immunodeficiency-virus type-1 Tar DNA-sequence motifs. J Virol 1995;69:3584–3596. [PubMed: 7745706]

Jellinger KA. Neuropathological spectrum of synucleinopathies. Mov Disord 2003;18:S2–S12. [PubMed: 14502650]

Johnson BS, McCaffery JM, Lindquist S, Gitler AD. A yeast TDP-43 proteinopathy model: exploring the molecular determinants of TDR-43 aggregation and cellular toxicity. Proc Natl Acad Sci USA 2008;105:6439–6444. [PubMed: 18434538]

Kabashi E, Valdmanis PN, Dion P, et al. TARDBP mutations in individuals with sporadic and familial amyotrophic lateral sclerosis. Nat Genet 2008;40:572–574. [PubMed: 18372902]

Lin W-L, Dickson DW. Ultrastructural localization of TDP-43 in filamentous neuronal inclusions in various neurodegenerative diseases. Acta Neuropathol 2008;116:205–213. [PubMed: 18607609]

Mosaheb S, Thorpe JR, Hashemzadeh-Bonehi L, Bigio EH, Gearing M, Cairns NJ. Neuronal intranuclear inclusions are ultrastructurally and immunologically distinct from cytoplasmic inclusions of neuronal intermediate filament inclusion disease. Acta Neuropathol 2005;110:360–368. [PubMed: 16025283]

Mukherjee OP, Pastor P, Cairns NJ, et al. HDDD2 is a familial frontotemporal lobar degeneration with ubiquitin-positive, taunegative inclusions caused by a missense mutation in the signal peptide of progranulin. Ann Neurol 2006;60:314–322. [PubMed: 16983685]

Mukherjee O, Wang J, Gitcho M, et al. Molecular characterization of novel progranulin (GRN) mutations in frontotemporal dementia. Hum Mutat 2008;29:512–521. [PubMed: 18183624]

Nakashima-Yasuda H, Uryu K, Robinson J, et al. Co-morbidity of TDP-43 proteinopathy in Lewy body related diseases. Acta Neuropathol 2007;114:221–229. [PubMed: 17653732]

Neumann M, Sampathu DM, Kwong LK, et al. Ubiquitinated TDP-43 in frontotemporal lobar degeneration and amyotrophic lateral sclerosis. Science 2006;314:130–133. [PubMed: 17023659]

Seelaar H, Schelhaas HJ, Azmani A, et al. TDP-43 pathology in familial frontotemporal dementia and motor neuron disease without progranulin mutations. Brain 2007;130:1375–1385. [PubMed: 17360763]

Sreedharan J, Blair IP, Tripathi VB, et al. TDP-43 mutations in familial and sporadic amyotrophic lateral sclerosis. Science 2008;319:1668–1672. [PubMed: 18309045]

Thorpe JR. Hajibagheri MA. The application of LR gold resin for immunogold labeling. Chapter 6. Electron microscopy methods and protocols Methods in molecular biology Series 1999;vol 117:99–110.

Thorpe JR, Morley SJ, Rulten SL. Utilising the peptidyl- prolyl-cis-trans isomerase Pin1 as a probe of its phosphorylated target proteins: examples of binding to nuclear proteins in a human kidney cell line and to Tau in Alzheimer's diseased brain. J Histochem Cytochem 2001;49:97–108. [PubMed: 11118482]

Thorpe JR, Mosaheb S, Hashemzadeh-Bonehi L, et al. Shortfalls in the peptidyl-prolyl cis-trans isomerase protein Pin1 in neurons are associated with frontotemporal dementias. Neurobiol Dis 2004;17:237–249. [PubMed: 15474361]

Uryu KN-Y, Forman H, Kwong MS, et al. Concomitant TARDNA-binding protein 43 pathology is present in Alzheimer disease and corticobasal degeneration but not in other tauopathies. J Neuropath Exp Neurol 2008;67:555–564. [PubMed: 18520774]

Zuccato E, Buratti E, Stuani C, Baralle FE, Pagani F. An intronic polypyrimidine-rich element downstream of the donor site modulates cystic fibrosis transmembrane conductance regulator exon 9 alternative splicing. J Biol Chem 2004;279:16980–16988. [PubMed: 14966131]

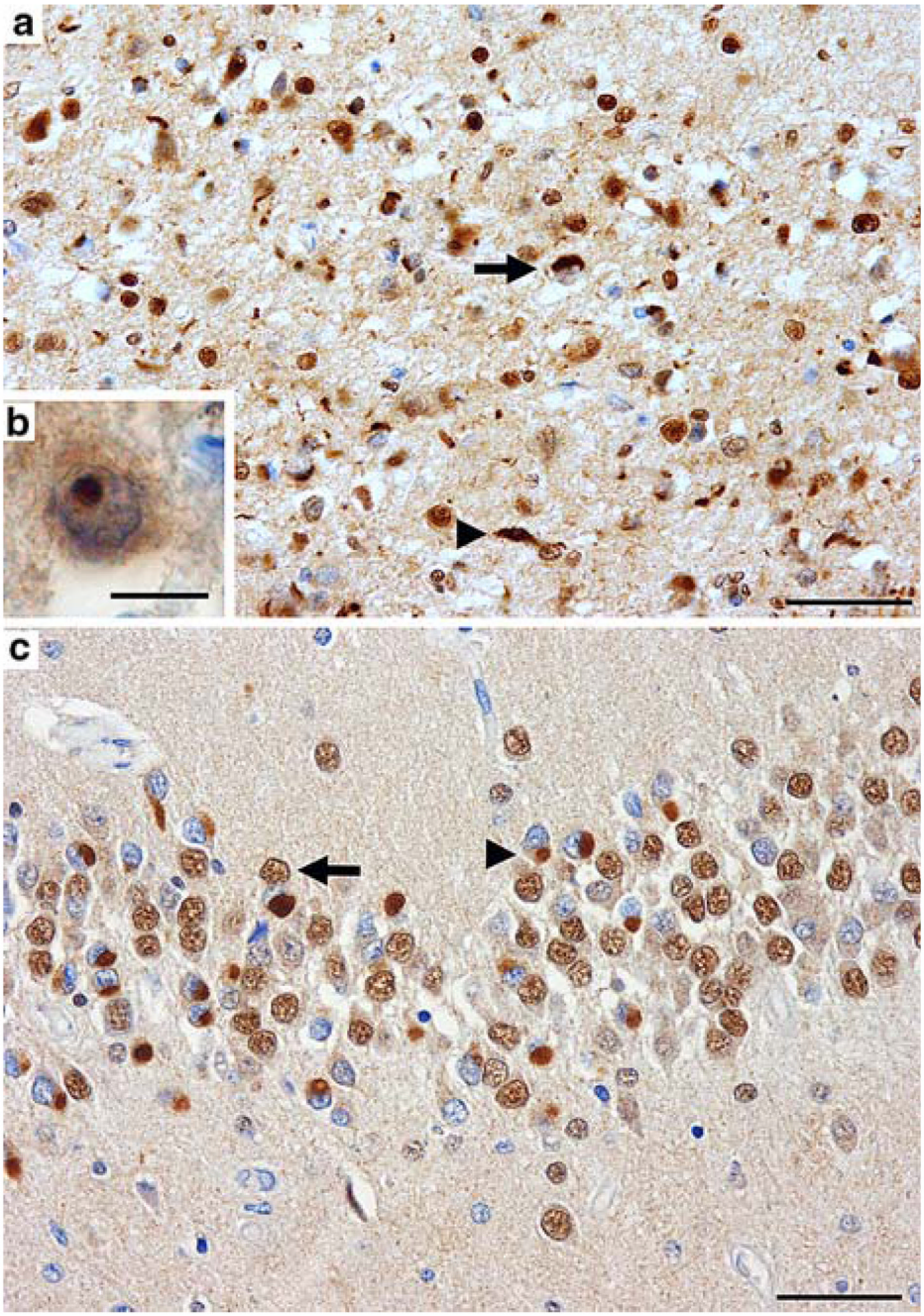

Fig. 1.

TDP-43-immunoreactive NCIs, DNs and an NII in the frontal lobe (**a**, **b**) and hippocampus (**c**) of FTLD with TDP-43 proteinopathy. **a** Neuronal loss, gliosis, microvacuolation, and numerous NCIs (*arrow*), DNs (*arrowhead*), and an NII (**b**) in superficial laminae of the middle frontal gyrus. **c** Numerous NCIs are present within the granule neurons of the dentate fascia. In unaffected neurons (*arrow*), the nucleus is labelled by anti-TDP-43 antibodies. In a neuron with an NCI (*arrowhead*), the nucleus is unlabelled by anti-TDP-43 antibodies, indicating abnormal translocation of TDP-43 between the nucleus and cytoplasm. (*NCI* neuronal cytoplasmic inclusion, *DN* dystrophic neurite, *NII* neuronal intranuclear inclusion). TDP-43 immunohistochemistry; *bars* (**a**) and (**c**) 50 μm; (**b**) 10 μm

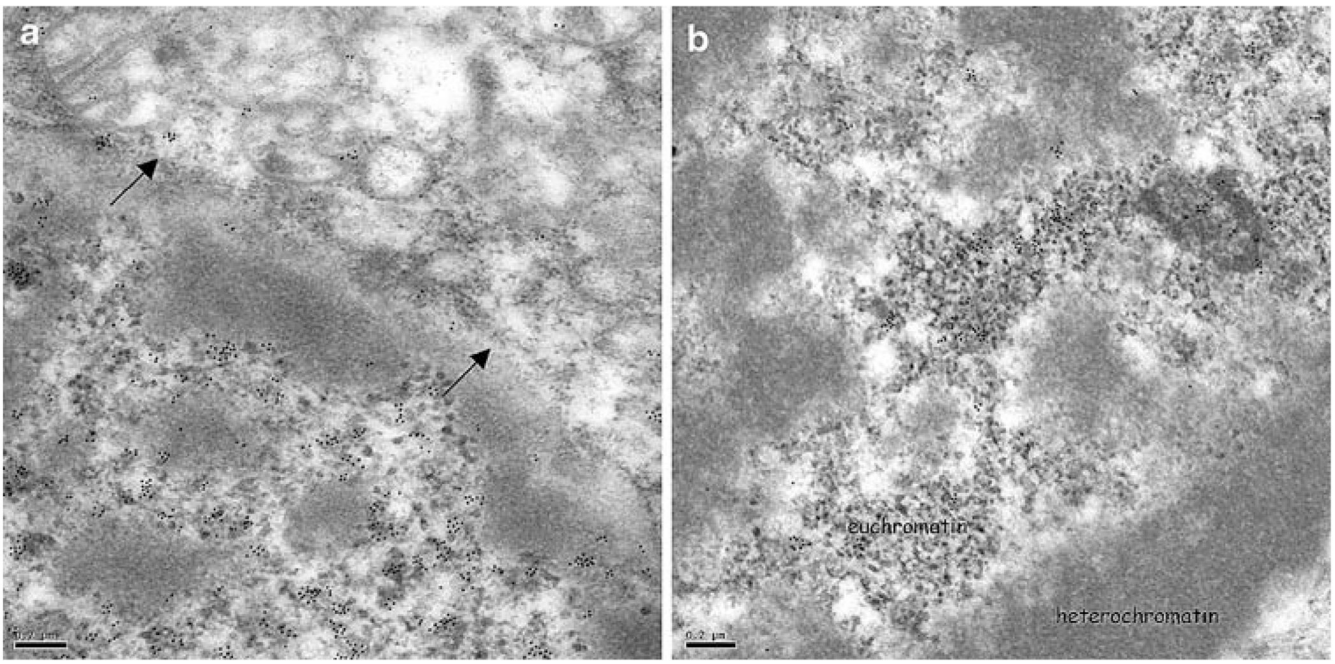

Fig. 2.

Normal brain immunogold labelling with anti-TDP-43 antibodies. TDP-43 epitopes are predominantly nuclear (**a** *arrows* demarcate the nuclear envelope) and are associated with regions of euchromatin within the nucleus (**a**, **b**). TDP-43 transmission immunogold electron microscopy. *Bars* 0.2 μm

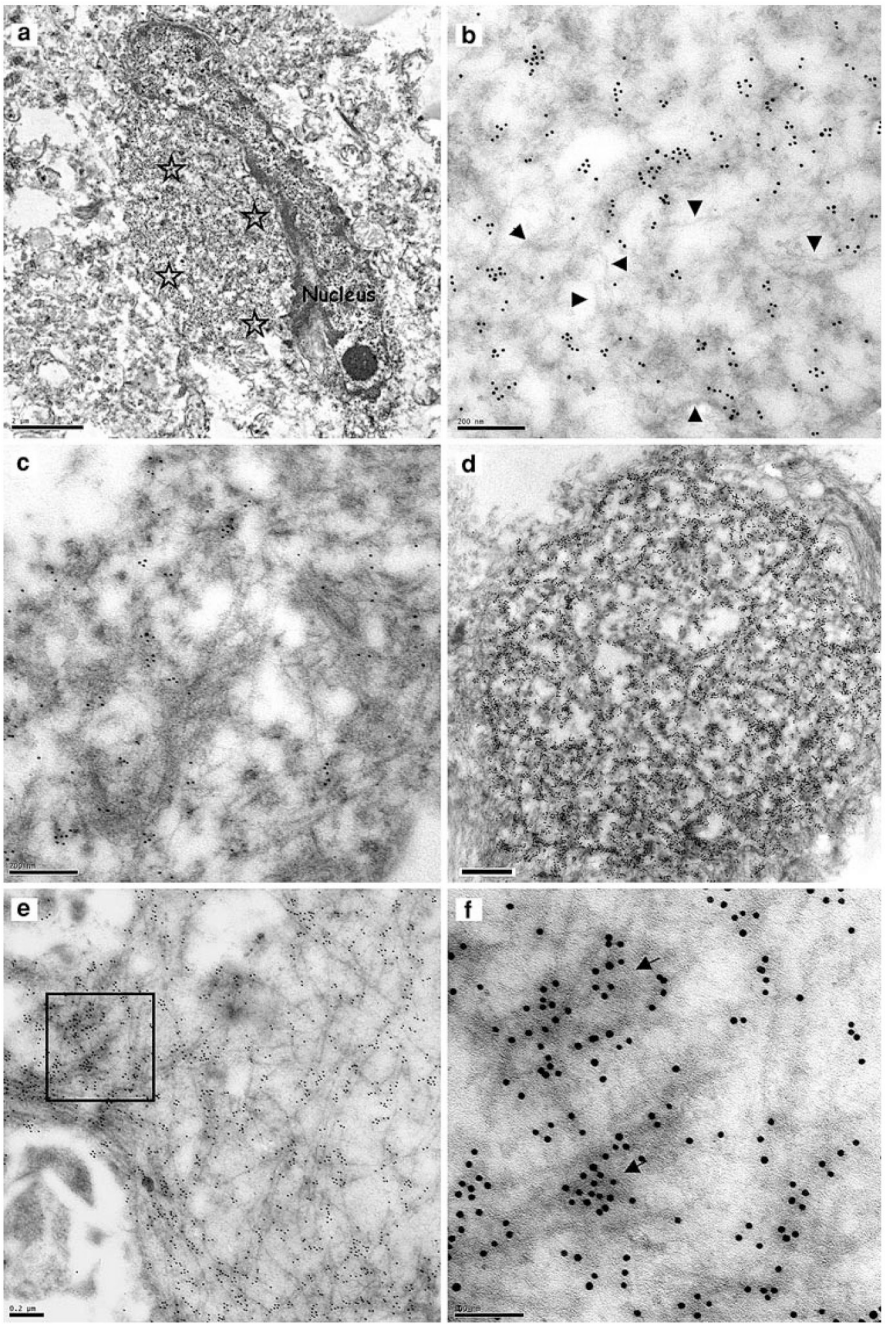

Fig. 3.

Neuronal cytoplasmic inclusions. TDP-43-immunoreactive NCIs in sporadic and familial cases of FTLD with TDP-43 proteinopathy. **a** Low power image of a neuron with an ovoidal, perikaryal, cytoplasmic inclusion (*asterisks* denote the inclusion area), **b** Portion of the TDP-43-labelled inclusion in (**a**). The inclusion comprises a granular component and fine, wispy filamentous regions which are not labelled significantly for TDP-43 (*arrowheads*); **c** A part of another NCI with a more pronouncedly fibrillary appearance, which is relatively lightly labelled. As in **b** the more fibrillary areas are not so intensely labelled, **d** A spherical NCI with a dense, predominantly granular, component has numerous TDP-43 epitopes, **e** A predominantly fibrillary NCI with intense TDP-43 positivity, **f** Enlarged view of the boxed

area in (**e**). The more intense anti-TDP-43 labelling is over the dense granular regions of the inclusion (*arrows*). TDP-43 transmission immunogold electron microscopy. *Bars* 2 μm (**a**), 0.2 μm (**b**, **c**, **e**), 0.5 μm (**d**) and 0.1 μm (**f**)

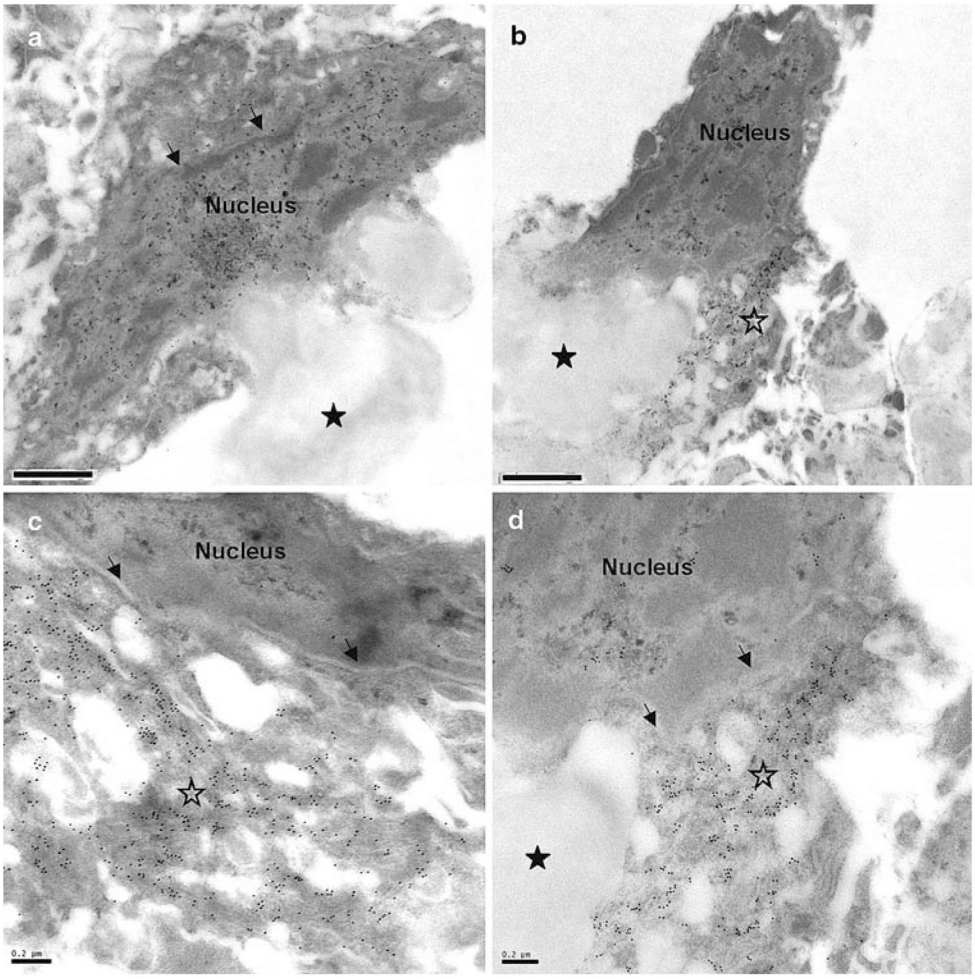

Fig. 4.

Neurons with cytoplasmic aggregates of TDP-43 show corresponding reduction in nuclear anti-TDP-43 labelling. **a** A neuron showing predominantly nuclear TDP-43 labelling, **b** A neuron showing accumulation of TDP-43 labelling in the perikaryal cytoplasm (*unfilled asterisk*), **c** Another example of a neuron showing perikaryal cytoplasmic accumulation of TDP-43, **d** Enlarged part of the neuron in (**b**). There are very low levels of TDP-43 labelling in the nucleus in (**b**), (**c**) and (**d**) compared with the nucleus in (**a**); compare with the normal brain neuronal nuclear TDP-43 labelling in Fig. 2. Annotations: *Arrows* demarcate the nuclear envelope, *unfilled asterisks* denote perikaryal cytoplasmic regions heavily labelled for TDP-43, *filled asterisks* denote lipofuscin. **a–d** case 106–69. TDP-43 transmission immunogold electron microscopy. *Bars* 1 μm (**a**, **b**) and 0.2 μm (**c**, **d**)

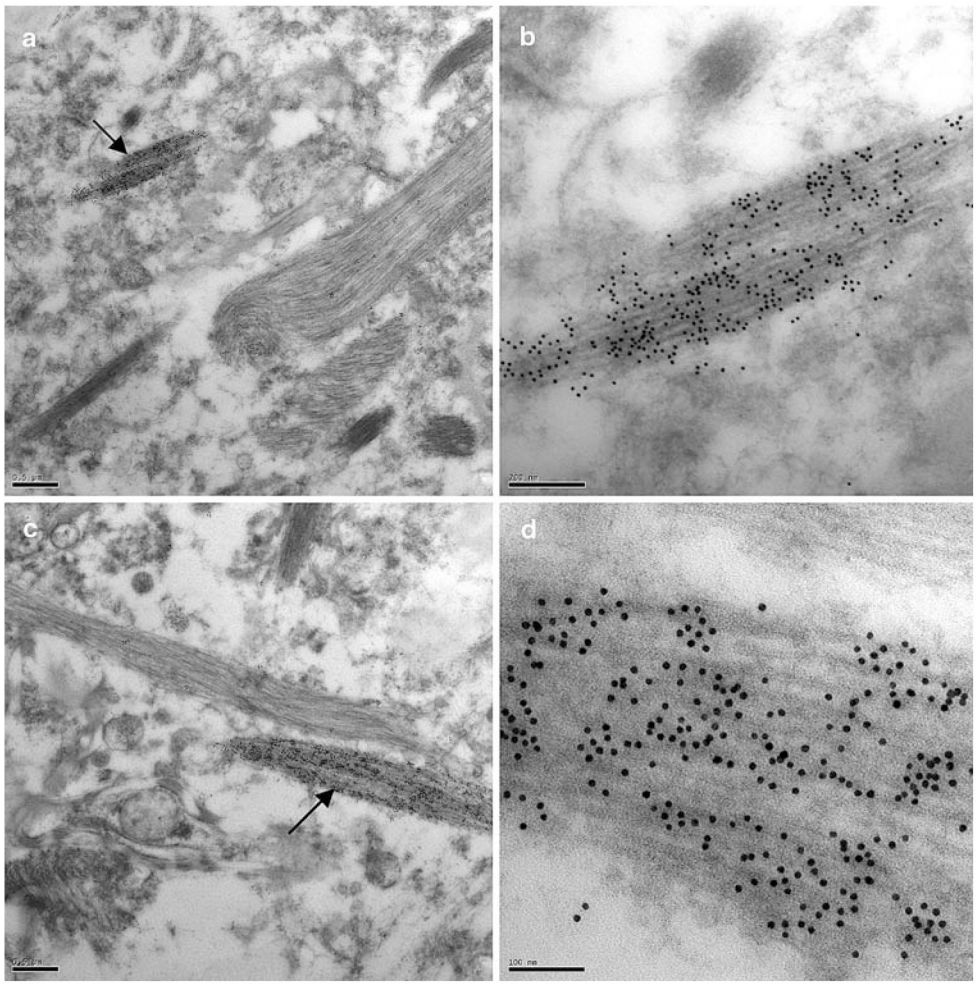

Fig. 5.

TDP-43 epitopes are present in a subset of neurites. **a** A neurite heavily decorated with anti-TDP-43 antibodies (*arrow*), adjacent to unlabelled, probably glial, processes, **b** Enlarged view of the TDP-43-labelled neuritic process in a, **c** A heavily TDP-43-immunolabelled neuritic process (*arrow*), alongside an unlabelled (glial) process, **d** High power electron micrograph of the TDP-43-labelled neuritic process arrowed in (**c**). (case 106–69). TDP-43 transmission immunogold electron microscopy. *Bars* 0.5 μm (**a**, **c**), 0.2 μm (**b**) and 0.1 μm (**d**)

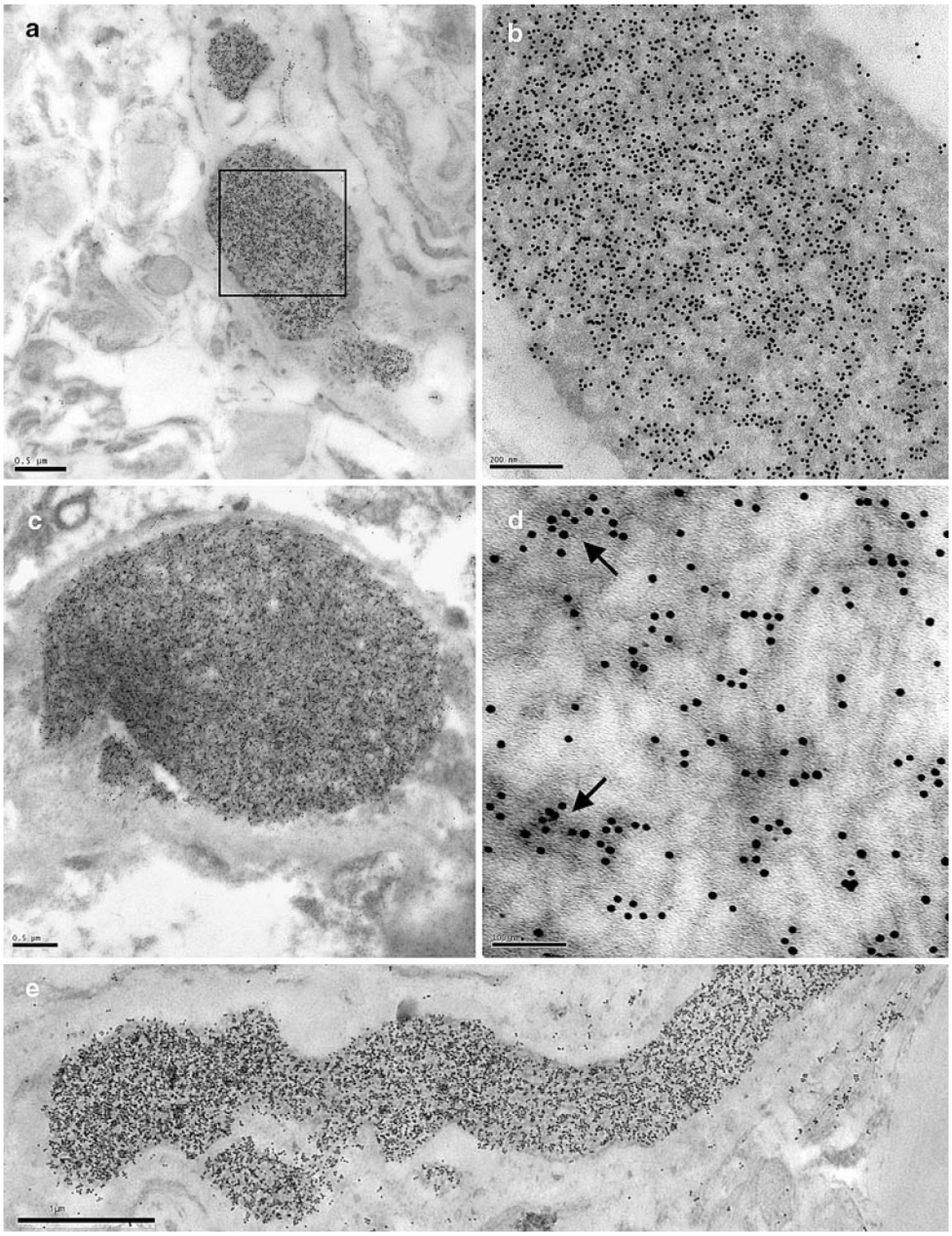

Fig. 6.

TDP-43-labelled dystrophic neurites. **a** A transverse section of a dense, swollen, heavily TDP-43-labelled dystrophic neurite, **b** Enlarged view of the boxed area in (**a**), **c** A swollen dystrophic neurite with a more fibrillar appearance, **d** Enlarged view of a portion of the dystrophic neurite in (**c**). The inclusion contains a fibrillary and granular component (*arrows*), the latter being more intensely labelled with anti-TDP-43 antibodies, **e** A dystrophic neurite in a serial section labelled with antiubiquitin antibodies. (**a–e**: case 106–69) TDP-43 and ubiquitin transmission immunogold electron microscopy. *Bars* 0.5 μm (**a**, **c**), 0.2 μm (**b**), 0.1 μm (**d**) and 1 μm (**e**)

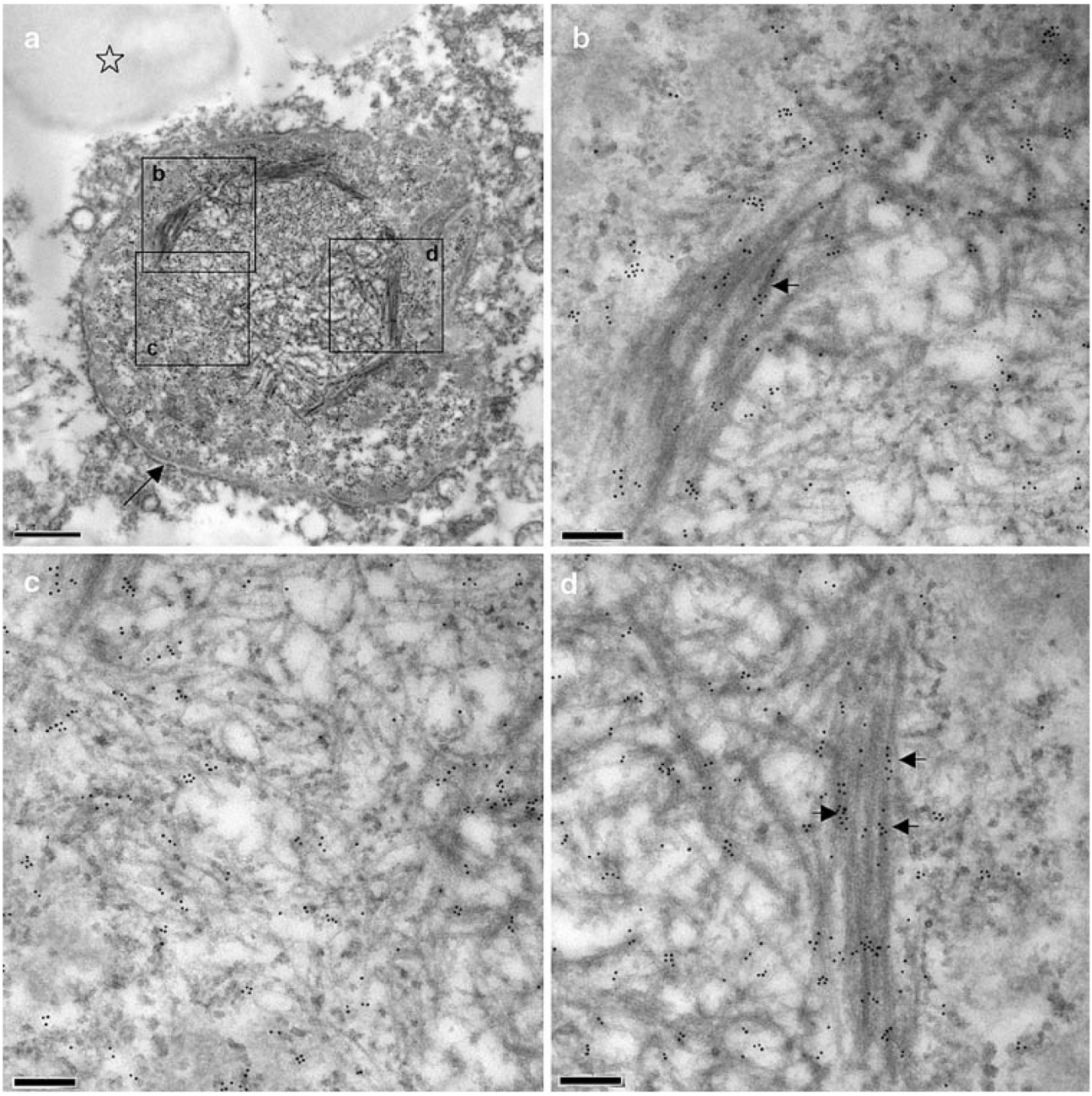

Fig. 7.

A neuronal intranuclear inclusion. A TDP-43-immunoreactive NII found in the superficial laminae of the frontal neocortex of a case of FTLD with TDP-43 proteinopathy. **a** Low power electron micrograph of NII (the *arrow* indicates the nuclear envelope and the *asterisk* identifies a lipofuscin granule), **b**, **c** and **d** High power electron micrographs of the corresponding boxed areas in (**a**). *Arrows* in **b** and **d** indicate TDP-43 labelling along the denser, broader fibrils of the inclusion (**a–d**: case 101–49). TDP-43 transmission immunogold electron microscopy. *Bars* 1 μm (**a**) and 0.2 μm (**b–d**)

Table 1

Demographic details of FTLD-U cases

Case no.	Gender	Age at death (years)	Familial/ sporadic	*GRN* mutation	Postmortem interval (h)	Cause of death	Neuropathologic subtype
100–57	Female	67	Familial	c.4068 G > A HDDD2 family	24	Inanition	FTLD-U type 3
106–69	Male	80	Familial	Deletion of exon 7; c.5913 A > G	12	Inanition	FTLD-U type 3
105–20	Female	84	Sporadic	None	10	Inanition	FTLD-U type 3
104–10	Female	78	Sporadic	None	4.4	Congestive heart failure	FTLD-U type 2
106–38	Male	66	Sporadic	None	7	Respiratory failure	FTLD-U type 2
101–49	Female	73	Sporadic	None	23.5	Pulmonary emboli	FTLD-U type 2

J Neural Transm. Author manuscript; available in PMC 2009 December 6.

Table 2

TDP-43-immunoreactive fibril analyses

Case no.	Heritability	FTLD-U subtype	NCI	DN	NII
100–57	F	3	6.9 nm (3.6–8)	9.0 nm (4.6–14)	n.a.
106–69	F	3	11.0 nm (6.1–15.6)	11.6 nm (7.9–15.6)	n.a.
105–20	S	3	10.2 nm (7.6–10.8)	n.a.	n.a.
104–10	S	2	9.0 nm (6.3–12.4)	9.6 nm (8.1–11.5)	n.a.
106–38	S	2	n.a.	10.4 nm (8.9–12.6)	n.a.
101–49	S	2	8.7 nm (5.7–11.6)	n.a.	Broad: 24.1 nm (10.6–49.8) Medium: 16.6 nm (9.0–26.5) Fine: 11.9 nm (9.7–16.0)

Fibril sizes are expressed as mean (range)

F familial, *S* sporadic, *NCI* neuronal cytoplasmic inclusion, *DN* dystrophic neurite, *NII* neuronal intranuclear inclusion

Table 3

Granular and filamentous components of neuronal inclusions of FTLD with TDP-43 proteinopathy

Case no	Diagnosis	Heritability	FTLD-U subtype	NCI			DN			NII
				G and F	G > F	F > G	F	G	G and F	F > G
100–57	FTLD-U	AD	3	+	−	−	+	−	−	n.a.
106–69	FTLD-U	AD	3	+	−	+	+	+	+	n.a.
105–20	FTLD-U	S	3	+	−	−	n.a.	n.a.	n.a.	n.a.
104–10	FTLD-U	S	2	+	+	−	+	−	−	n.a.
106–38	FTLD-U	S	2	n.a.	n.a.	n.a.	+	−	−	n.a.
101–49	FTLD-U	S	2	+	−	−	n.a.	n.a.	n.a.	+

Heritability: *AD* autosomal dominant, *S* sporadic, *G* and *F* granular and fibrillar components within inclusions, *G > F*, inclusions with pre-dominantly granular (*G*) component and fibrils (*F*) a minor component, *F > G* inclusions with predominantly fibrillar components and minor granular component, + TDP-43-immunoreactive inclusions as visualised by immunogold labelling, *n.a.* inclusion type not available